Fibers and Polymers 2013, Vol.14, No.6, 909-914 DOI 10.1007/s12221-013-0909-6

Effect of Degree of Polymerization on the Mechanical Properties of Regenerated Cellulose Fibers Using Synthesized 1-Allyl-3-methylimidazolium Chloride

Su-jin Kim and Jinho Jang*

Department of Nano-Bio Textile Engineering, Kumoh National Institute of Technology, Gumi 730-701, Korea

(Received February 2, 2012; Revised August 19, 2012; Accepted November 20, 2012)

Abstract: 1-Ally-3-methylimidazolium chloride ([AMIM]Cl) was successfully synthesized and was used as a green spinning solvent for cellulose. The celluloses of various degrees of polymerization (*DP*) were dissolved in the [AMIM]Cl to obtain 5 % (w/w) cellulose solutions, which were regenerated to cellulose fibers through wet spinning process. Of three different regenerated cellulose fibers with different *DP*s, a *DP* of 2,730 was gave the strongest regenerated fiber without drawing having a tensile strength of 177 MPa and an elongation at break of 9.6 % respectively, indicating that celluloses of higher molecular weight can be entangled and oriented more easily. Also maximum draw ratio of the as-spun fibers increased from 1.2 to 1.7 with increasing degree of polymerization leading to a tensile strength and modulus of 207 MPa and 48 GPa, respectively. Particularly the tensile modulus was substantially higher than those of lyocell and high performance viscose fibers of 20 GPa or less. The higher *DP* of pristine cellulose was critical in increasing the mechanical properties such as tensile strength and elongation at break of the as-spun fibers coupled with higher tensile modulus after drawing.

Keywords: Cellulose, Ionic liquid, [AMIM]Cl, Wet-spinning process, Mechanical properties

Introduction

The unstable supply of fossil fuels and the emergence of global warming have reawaken a strong interest in pursuing alternative and renewable polymeric materials [1]. Cellulose constitutes the most abundant biorenewable and biodegradable polymer resource in the world, with an annual yield of over 10^{10} ton. However, it is not wise to convert edible crops or vegetables into raw materials. The materials and energy should be extracted from inedible biomass, such as cereal straws, corn bagasse, recycled fabrics, and papers. For efficient conversion, it is necessary to dissolve under mild reaction conditions. However, because of their stiff molecules and close chain packing via numerous molecular hydrogen bonds, it is extremely difficult to dissolve cellulose in water and most common organic solvents [2-7]. To date, only a limited number of non-derivatizing solvent systems for cellulose have been found such as *N,N*-dimethylacetamide/lithium chloride (DMAc/LiCl) [8,9], *N*-methyl-2-pyrrolidine/lithium chloride (NMP/LiCl) [10], dimethyl sulfoxide/paraformaldehyde (DMSO/PF) [11], and molten salt hydrates [12,13]. However, these solvents have some limitations due to their cost, volatility, toxicity, instability, and recovery issues. Among the cellulose solvents, the *N*-methyl-morpholine-*N*-oxide/water (NMMO/H_2O) system is the solely applied solvent in industrial operations, regardless of the disadvantages such as the demand for high dissolving temperature, cellulose degradation, and its high cost [7,14].

Room-temperature ionic liquids (ILs) are composed of inorganic anions and organic cations including imidazolium, pyridinium, pyrrolidinium, ammonium, and phosphonium, which melt at temperatures lower than 100 °C. ILs are considered as desirable green solvents and they have been used to replace organic solvents in wide ranges of traditional applications due to their advantages such as reduction or prevention of chemical waste, the enhanced safety of chemical processes and products [15-17]. Recently, ILs has been used to dissolve native celluloses without derivation in high concentrations using 1-butyl-3-methylimidazolium chloride ([BMIM]Cl), 1-ethyl-3-methylimidazolium chloride ([EMIM]Cl), 1-allyl-3-methylimidazolium chloride ([AMIM]Cl), 1-ethyl-3-methylimidazolium acetate ([EMIM]OAc) [7,18-20]. In comparison with [BMIM]Cl, [EMIM]Cl, [EMIM]OAc, the smaller cation size of $[AMIM]^+$ in [AMIM]Cl due to three carbon atoms and a double bond of allyl group in N-substituted methylimiazonium cation results in lower melting point and viscosity [21,22].

In this study, the [AMIM]Cl was synthesized from methylimidazole and allyl chloride, which was applied as a green solvent for three different types of celluloses. The cellulose/[AMIM]Cl solution was spun by wet spinning and the mechanical properties of the regenerated cellulose fibers were analyzed in relation with the degree of polymerization (*DP*) of the celluloses to investigate the effect of *DP* on the mechanical properties of the regenerated cellulose fibers.

Experimental

Materials

The cellulose samples used in this study include microcrystalline cellulose (MCC), filter paper, and cotton fabrics. The viscosity-average degree of polymerization (*DP*) of the three cellulose materials was 1740, 2310, and 2730, respectively, which was determined using an Ubbelohde viscometer in 9 % (w/w) *N,N*-dimethylacetamide/lithium chloride [8]. The cotton fabrics (50.0 g/m^2) were provided by Sombe, while

---

*Corresponding author: jh.jang@kumoh.ac.kr

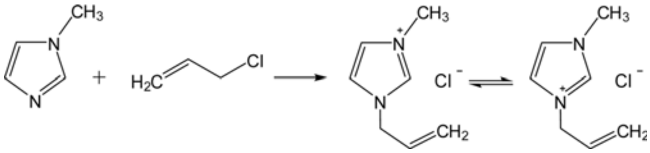

Figure 1. Synthesis of [AMIM]Cl.

MCC (0.6 g/m*l*) and filter paper (137.8 g/m^2) were purchased from Aldrich and Hyundai micro, respectively. 1-Methylimidazole and allyl chloride supplied by Aldrich were used for the synthesis of [AMIM]Cl.

Synthesis of [AMIM]Cl

1-Methylimidazole and allyl chloride at a molar ratio of 1: 1.25 were added to a flask fitted with a reflux condenser at 55 °C for 8 h under stirring. The unreacted chemical reagents and other impurities such as water were removed by vacuum distillation, and the obtained [AMIM]Cl is slightly amber (Figure 1).

Mass spectroscopy was used to measure the molecular weight of the synthesized [AMIM]Cl. Elemental analysis (2400 series II, Perkin Elmer) and ion chromatography (938 Advanced IC) were carried to measure the contents of carbon, hydrogen, nitrogen, and chlorine of the synthesized [AMIM]Cl. The molecular structures of the synthesized [AMIM]Cl was characterized by FT-IR (300E, JASCO) and 400 MHz ^{1}H NMR (Avance Digital 400, Bruker) using D_2O.

Dissolution and Spinning

Cellulose samples were cut into small pieces and dried at 60 °C for 1 h in a vacuum oven before use. The cellulose samples without pretreatment were added to the flask containing [AMIM]Cl at 110 °C for 1 h. The 5 wt% cellulose/[AMIM]Cl dope solution at 80 °C was transferred to a syringe, which was extruded through a needle with a diameter of 0.3 mm under pressured nitrogen to a coagulation bath of water at 25 °C. The fully coagulated fiber was extended to the breakage in secondary washing bath at 50 °C. The maximum draw ratio was determined by the maximum length of the elongated fiber before breakage to that of the as-spun finer. The spun and drawn fiber was washed with running water and vacuum dried.

Characterization of Regenerated Cellulose Fibers

The fiber samples were dried at 60 °C in a vacuum oven before use. The *DP* of original and regenerated celluloses was measured by an Ubbelohde viscometer in DMAc/LiCl [8]. FT-IR spectrometer (300E, JASCO) with KBr pellet was used to observe the molecular structure of original and regenerated celluloses. The IR crystallinity index (*CI*(IR)) was calculated by equation (1).

$$CI\,(\mathrm{IR}) = A_{1372\mathrm{cm}^{-1}} / A_{2990\mathrm{cm}^{-1}} \tag{1}$$

Wide-angle X-ray diffraction (WAXD) measurements of the original and regenerated celluloses were performed on an X-MAX diffractometer (2000PC, Rigaku). Ni-filtered Cu Kα radiation (λ=1.54 Å) generated at a voltage of 40 kV and current of 150 mA was utilized at a scan speed of 2 °/min from 5 to 40 °. The crystallinity index (*CI*(WAXD)), crystallite size (*L*), and interplanar distance (*D*) were calculated by equations (2)-(4).

$$CI\,(\mathrm{WAXD}) = A_c / (A_c + A_m) \tag{2}$$

$$L = k\lambda / \beta\cos\theta \tag{3}$$

$$D = \lambda / 2\sin\theta \tag{4}$$

where A_c is area of crystalline phase (cellulose I: 2θ=14.8 °, 16.3 °, and 22.6 °, cellulose II: 2θ=12.1 ° and 20.0 °), A_m is area of amorphous phase (cellulose I: 2θ=20.1 °, cellulose II: 2θ=18.3 °), k is the Scherrer constant (0.94) and β is the full-width at half-maximum.

Moisture Regain Measurement

For moisture regain measurements, cellulose samples were dried at 60 °C for 1 h in a vacuum oven before use. All samples were conditioned for over 24 h in a standard atmosphere at 20±2 °C and 65±4 % relative humidity (RH) prior to tests.

Mechanical Properties of Regenerated Cellulose/[AMIM]Cl Fiber

The mechanical properties of the fibers were measured using a universal test machine (Instron series 4467, U.K.). The sample length was 2 cm and the extension rate was set at 0.4 cm/min. Ten samples or more were measured to average the tensile properties such as strength, modulus and elongation at break.

Morphology of Regenerated Cellulose Fiber

The surfaces and cross section of the regenerated cellulose fibers were observed with a scanning electron microscope (JSM-6580F, JEOL). The fibers were frozen in liquid nitrogen and fractured before the observation.

Results and Discussion

Characterization of the Synthesized [AMIM]Cl

As a commercial chemical, the [AMIM]Cl has been as expensive as 10,000 Wons per gram. To reduce the solvent cost, the [AMIM]Cl was synthesized directly from 1-methylimidazole and allyl chloride in our laboratory. The yield of the synthesized [AMIM]Cl was 96.5 %. Through the synthesis of solvents, we can reduce its cost as much as thirty times.

The [AMIM]Cl consists of an imidazolium cation and a chloride anion. From the mass spectrum of the synthesized solvent, the intact cation of the [AMIM]Cl was located at m/z 123.2, which was in very good agreement with the theoretical molecular weight of [AMIM]$^+$ ion. The elemental analysis and ion chromatography results of [AMIM]Cl were given in Table 1. The elemental contents of the calculated and the found showed no significant differences. To clarify the structure of synthesized [AMIM]Cl, ^{1}H NMR studies were carried out before and after the synthesis (Figure 2). The synthesized [AMIM]Cl showed both 1-methylimidazole and allyl chloride peaks at comparable peak area and new doublet peaks at 4.81 ppm resulted from the covalent bond formation between allyl and imidazole groups. Figure 3 shows FT-IR spectrum of [AMIM]Cl. It can be seen that the C-H stretching and imidazolium ring bending were observed at 3078 cm^{-1} and 1571 cm^{-1} respectively, indicating the presence of the imidazolium ring. And the C=C stretching of allyl group also appeared at 1645 cm^{-1}. In addition, strong C-N stretching appeared at 1166 cm^{-1}.

Table 1. Elemental analysis and ion chromatograph of [AMIM]Cl

		C (wt%)	H (wt%)	O (wt%)	Cl (wt%)
[AMIM]Cl	Calculated	53.0	6.9	17.7	22.4
	Found	52.1	7.1	17.9	23.3

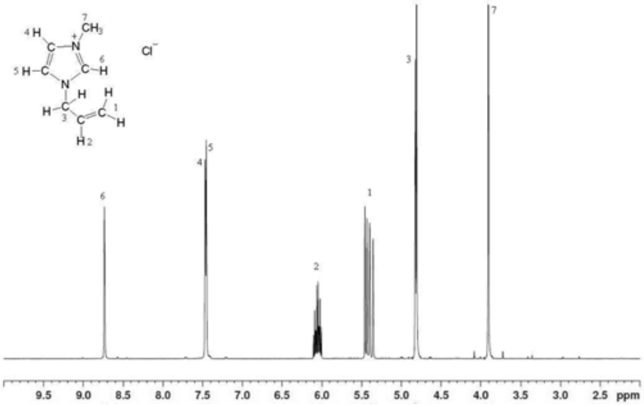

Figure 2. ^{1}H NMR spectra of the synthesized [AMIM]Cl.

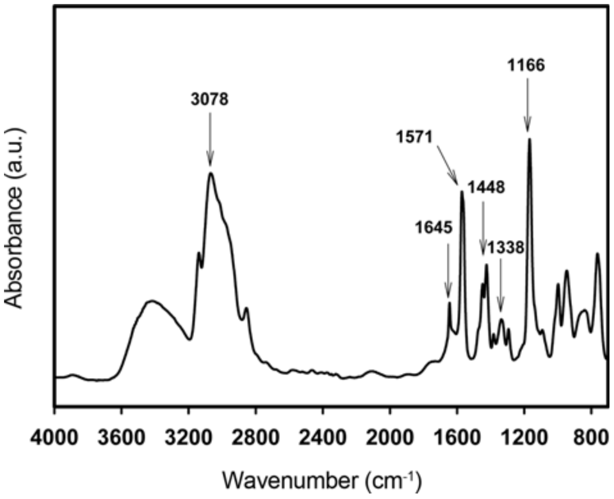

Figure 3. FT-IR spectrum of the synthesized [AMIM]Cl.

Molecular Structures of the Regenerated Cellulose Fiber

FT-IR spectra of the cotton and regenerated fibers from cotton were shown in Figure 4. The two samples showed similar spectrum, indicating that no chemical reaction occurred during the dissolution and coagulation processes. For the cotton, the peak was separated sharply to five peaks from 1450 to 1250 cm^{-1}. However, the peak of regenerated fibers centered broadly at 1377 cm^{-1} [23]. The regenerated fibers had more weakened absorption band at 1442 cm^{-1} compared to the CH_2 scissoring peak at 1431 cm^{-1} for the original cotton, resulting from the destruction of the intramolecular hydrogen bond at C_6 [7]. Also a new C-O stretching vibration in the amorphous region at 897 cm^{-1} was strengthened in the regenerated cellulose fiber. FT-IR spectra were used to calculate IR crystallinity index [24]. The crystallinity index of original cellulose sources showed that the filter paper was the highest crystallinity index as 0.51 and the MCC was the lowest crystallinity index as 0.45 (Table 2). After dissolution and spinning processes, the crystallinities of original celluloses diminished substantially as shown in Table 3. All the regenerated fibers from different cellulose sources showed similar

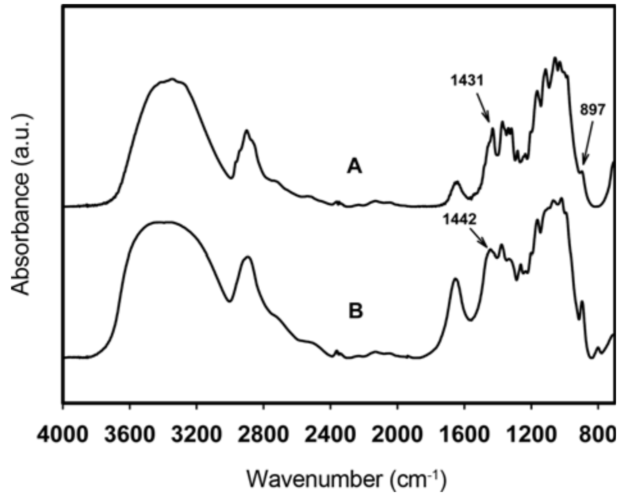

Figure 4. FT-IR spectra of (A) cotton and (B) regenerated cellulose fibers from cotton/[AMIM]Cl solution.

Table 2. Characteristics of original cellulose sources

	MCC	Filter paper	Cotton
DP	1,740	2,310	2,730
CI (IR)	0.45	0.51	0.49
CI (WAXD)	0.71	0.90	0.88
Crystal size (nm)	6.71	8.29	10.19
d-spacing (Å)	3.93	3.93	3.96
Moisture regain (%)	9.0	7.9	8.1

Table 3. Characteristics of of regenerated cellulose fibers

	Regenerated cellulose fibers		
	MCC	Filter paper	Cotton
DP	1,430	1,720	2,140
CI (IR)	0.17	0.18	0.20
CI (WAXD)	0.44	0.45	0.45
Crystal size (nm)	2.23	2.31	2.32
d-spacing (Å)	4.62	4.41	4.33
Fineness (tex)	10.7	11.3	12.0
Moisture regain (%)	10.8	10.5	10.5

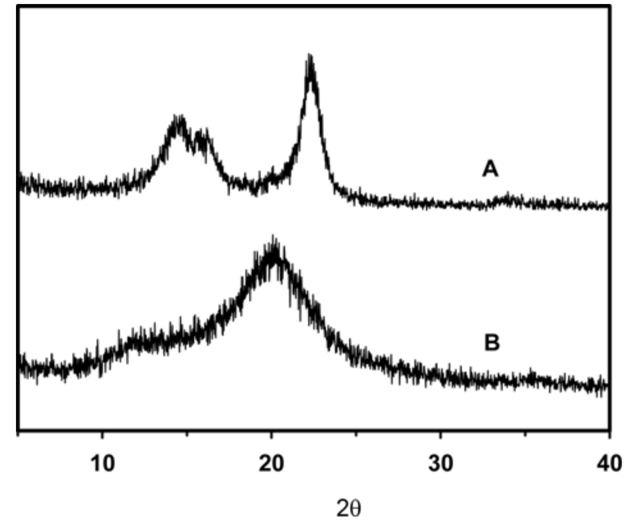

Figure 5. WAXD patterns of (A) cotton and (B) regenerated cellulose fibers from cotton/[AMIM]Cl solution.

crystallinity. However, it makes a little difference depending on *DP*. The regenerated fibers from cotton which was the highest *DP* showed slightly higher crystallinity than regenerated fibers from filter paper and MCC.

Figure 5 shows the X-ray diffraction patterns of the pristine celluloses and regenerated cellulose fibers. The pristine celluloses such as cotton, filter paper, and MCC are characterized to cellulose I as indicated by the typical diffraction peaks at 2θ of 14.8 °, 16.3 °, and 22.6 °, while the main peaks of crystal structure of cellulose II were reported at 19.9 ° and 21.6 ° [25]. After dissolution and subsequent coagulation with water, the regenerated cellulose exhibits the diffraction patterns of cellulose II at 20.3 ° and 21.6 °. The transformation from cellulose I to cellulose II has been known to occur after the dissolution in [AMIM]Cl and regeneration [26,27]. The crystallinity index and crystal size of regenerated fibers were lower than the original celluloses as summarized in Tables 2 and 3. The IL easily broke the intermolecular and intramolecular hydrogen bonds and destroyed the original crystalline structure during the dissolution process. Also, all the regenerated cellulose fibers from different type of celluloses showed similar crystallinity index irrespective of their sources because the [AMIM]/cellulose solutions experienced same dissolution and spinning conditions. However, the *d*-spacing decreased and crystal size increased with increasing degree of polymerization of celluloses, suggesting the stronger molecular interactions between longer cellulose chains.

The moisture regain was measured to investigate the influence of moisture uptake on the internal hydrophilic space of cellulose. The moisture regain was related to the content of amorphous region. The filter paper of the highest crystallinity was the lowest moisture regain as 7.9 %, and MCC of the lowest crystallinity was the highest moisture regain as 9.0 % (Table 2). After dissolution and spinning, the regenerated cellulose fibers of low crystallinity had higher moisture regain than original cellulose sources (Table 3). All the regenerated cellulose fibers from different type of celluloses showed similar moisture regain due to their similar crystallinity.

Mechanical Properties of the Regenerated Cellulose Fiber

The *DP* of regenerated cellulose fibers is intimately related with mechanical properties and drawing ability. After dissolution and spinning, the *DP* of regenerated fiber obtained from solutions of cotton, filter paper and MCC significantly decreased compared with that of pristine celluloses by 24.6 %, 27.0 %, and 32.9 %, respectively.

The stress-strain curves for different *DP* of cellulose fibers under tensile loading are shown in Figure 6. And the effect of the *DP* on the mechanical properties and maximum draw ratio of regenerated fibers was shown in Figures 7 and 8. While the tensile modulus of all the regenerated cellulose fibers is nearly same as 11±0.3 GPa, the tensile strength and the elongation at break of the regenerated fibers increased from 127 MPa (1.0 g/d) to 207 MPa (1.6 g/d) and from 6.6 % to 9.6% with increasing *DP* of the celluloses respectively. The mechanical properties of as-spun fibers increased with

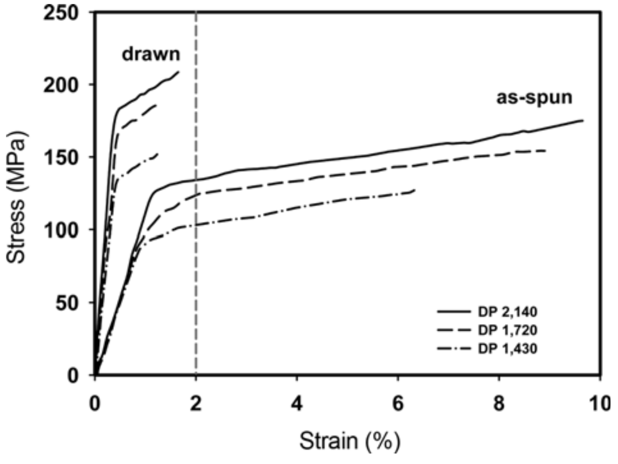

Figure 6. Stress-strain curves for regenerated cellulose fibers.

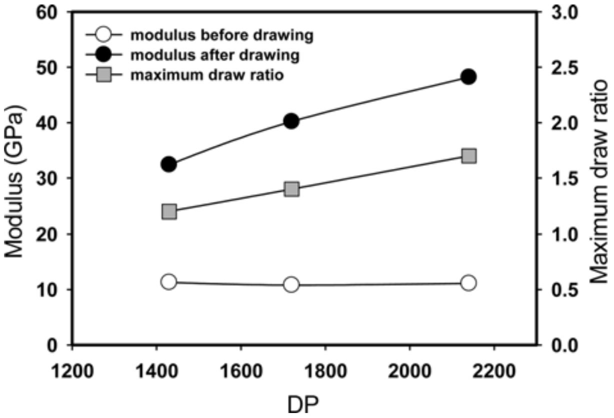

Figure 7. The effect of DP on draw ratio and modulus.

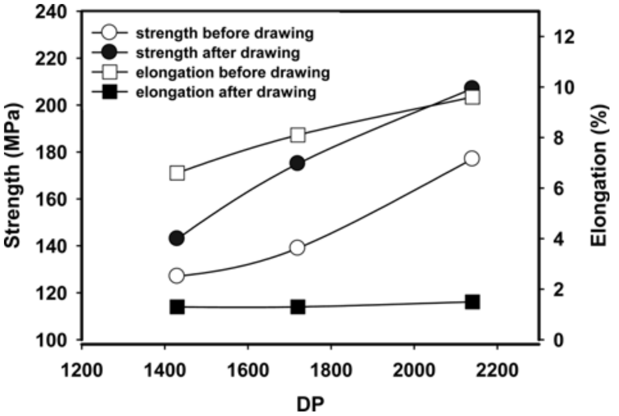

Figure 8. The effect of DP on strength and elongation.

additional drawing and the higher *DP* fiber can be drawn more than lower *DP* fiber as indicated by the maximum draw ratio, under the present drawing system, was proportionally increased from 1.2 to 1.7 with the increasing *DP* from 1,430 to 2,140 respectively. It may be resulted from that higher molecular weight chains can be entangled and withstand the external forces more efficiently. And the drawn fibers of the highest *DP* showed the highest tensile strength of 207 MPa (1.6 g/d) and a modulus of 48.2 GPa and a very low elongation of 1.5 %. The improved modulus and strength of the drawn fibers were coupled with the decreased elongation, which was probably caused by the increase of the orientation of the polymer chain along the filament axis induced by drawing. With drawing, the as-spun fibers with higher *DP* were found to have higher modulus and strength. Further works may be required to maximize the mechanical properties of the regenerated cellulose fiber by optimizing cellulose concentration and spinning conditions such as dope temperature and shear rate.

Morphology of Regenerated Cellulose Fiber

Figure 9 shows scanning electron microscopy photographs of the regenerated cellulose fibers from cotton cellulose. It can be clearly seen that the surfaces of the regenerated cellulose fibers were smooth without any obvious crevices or flaws with round cross section.

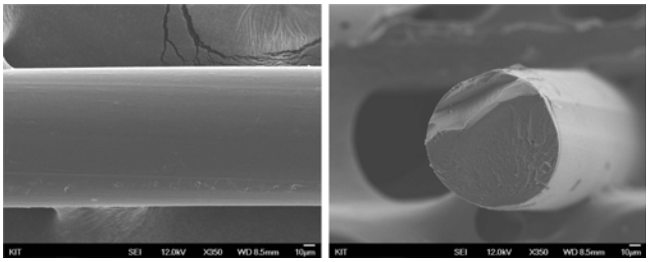

Figure 9. SEM images of the regenerated cellulose fiber from cotton/[AMIM]Cl solution.

Conclusion

In this study [AMIM]Cl was used as an ionic liquid solvent for cellulose and the regenerated cellulose fibers were prepared by a wet-spinning method. Under the current spinning conditions, celluloses of a *DP* up to 2,730 can be completely dissolved in the [AMIM]Cl and regenerated fibers with similar crystallinity and moisture regain were obtained after coagulation in water. The as-spun fibers showed a cellulose II crystal structure similar to Lyocell fibers. The draw ratio and mechanical properties of the regenerated fibers such as tensile strength and elongation at break were strongly dependent on the *DP* of the pristine celluloses. The cellulose fibers with a tensile strength of 177 MPa and a modulus of 11 GPa were successfully spun from cotton cellulose with a *DP* of 2,730. The drawn fibers based on cotton cellulose at a draw ratio of 1.7 showed a tensile strength of 207 MPa and a modulus of 48 GPa. The higher molecular weight of raw cellulose was critical in increasing the mechanical properties of the regenerated fibers such as tensile strength and elongation at break of the as-spun fibers coupled with their tensile modulus after drawing. The ionic liquid [AMIM]Cl could be utilized in a new environment friendly solvent for cellulose dissolution and spinning of a high modulus cellulose fibers.

Acknowlegements

This research was financially supported by the Ministry of Education, Science Technology (MEST) and National Research Foundation of Korea (NRF) through the Human Resource Training Project for Regional Innovation.

References

1. M. E. Himmel, S. Y. Ding, D. K. Johnson, W. S. Andey, M. R. Nimlos, J. W. Brady, and T. D. Foust, *Science*, **315**, 5813 (2007).

2. H. Ohno and Y. Fukaya, *Chem. Lett.*, **38**, 2 (2009).
3. D. Klemm, B. Heublein, H. P. Fink, and A. Bohn, *Angew. Chem. Int. Ed.*, **44**, 3358 (2005).
4. Y. Habibi, L. A. Lucia, and O. J. Rojas, *Chem. Rev.*, **110**, 3479 (2010).
5. T. Cai, H. Zhang, Q. Guo, H. Shao, and X. Hu, *J. Appl. Polym. Sci.*, **115**, 1047 (2010).
6. J. Mussig, "Industrial Applications of Natural Fibres; Structure, Properties and Technical Applications", pp.13-22, Wiley, Chichester, UK, 2010.
7. H. Zhang, J. Wu, J. Zhang, and J. He, *Macromolecules*, **38**, 8272 (2005).
8. C. L. McCormick, P. A. Callais, and B. H. Hutchinson, *Macromolecules*, **18**, 2394 (1985).
9. M. Terbojevich, A. Cosani, G. Conio, A. Ciferri, and E. Bianchi, *Macromolecules*, **18**, 640 (1985).
10. K. J. Edgar, K. M. Arnold, W. W. Blount, J. E. Lawniczak, and D. W. Lowman, *Macromolecules*, **28**, 4122 (1995).
11. J. F. Masson and R. S. J. Manley, *Macromolecules*, **24**, 5914 (1991).
12. S. Fischer, W. Voigt, and K. Fischer, *Cellulose*, **6**, 213 (1999).
13. K. Hattori, J. A. Cuculo, and S. M. Hudson, *J. Polym. Sci. Part A: Polym. Chem.*, **40**, 601 (2002).
14. J. P. Mikkola, A. Kirilin, J. C. Tuuf, A. Pranovich, B. Holmbom, L. M. Kustov, D. Y. Murzin, and T. Salmi, *Green Chem.*, **9**, 1229 (2007).
15. M. Freemantle, "An Introduction to Ionic Liquids", pp.1-11, RSC Publishing, Cambridge, UK, 2010.
16. D. M. Phillips, L. F. Drummy, D. G. Conrady, D. M. Fox, R. R. Naik, M. O. Stone, P. C. Trulove, H. C. D. Long, and R. A. Mantz, *J. Am. Chem. Soc.*, **126**, 14350 (2004).
17. V. A. Cocalia, K. E. Gutowski, and R. D. Rogers, *Chem. Rev.*, **250**, 755 (2006).
18. R. P. Swatloski, S. K. Spear, J. D. Holbrey, and R. D. Rogers, *J. Am. Chem. Soc.,* **124**, 4974 (2002).
19. B. Kosan, C. Michels, and F. Meister, *Cellulose*, **15**, 676 (2008).
20. H. Zang, Q. Su, Y. Mo, B. Cheng, and S. Jun, *Ultrason. Sonochem.*, **17**, 749 (2010).
21. Y. Fukaya, A. Sugimoto, and H. Ohno, *Biomacromolecules*, **7**, 3295 (2006).
22. T. Mizumo, E. Marwanta, N. Matsumi, and H. Ohno, *Chem. Lett*., **33**, 1360 (2004).
23. K. J. Kim and B. S. Yun, *J. Kor. Soc. Text. Eng. Chem.*, **23**, 177 (1986).
24. M. L. Nelson and R. T. O'Connor, *J. Appl. Poly. Sci*., **8**, 1325 (1964).
25. G. Cheng, P. Varanasi, C. Li, H. Liu, Y. B. Melnichenko, B. A. Simmons, M. S. Kent, and S. Singh, *Biomacromolecules*, **12**, 933 (2011).
26. S. Raymond, A. Kvick, and H. Chanzy, *Macromolecules*, **28**, 8422 (1995).
27. F. Kolpak and J. Blackwell, *Macromolecules*, **9**, 273 (1976).